Increasing variable stiffness actuator-response using an electromagnetic spring

Yang, Han Ping; Jang, Chau Shin; Van Der Kooij, Herman

DOI
10.1109/ICARM.2019.8834303

Publication date
2019

Document Version
Accepted author manuscript

Published in
Proceedings of the 4th IEEE International Conference on Advanced Robotics and Mechatronics (ICARM 2019)

Increasing Variable Stiffness Actuator-Response Using an Electromagnetic Spring*

Han-Ping Yang, Chau-Shin Jang, and Herman van der Kooij, *Member, IEEE*

***Abstract*—An electromagnetic spring-based variable stiffness actuator is a new concept with the potential to change stiffness faster than mechanical springs can; however, its nonlinear elastic property is a challenge in actuator design. In this paper, the torque response of a custom-made electromagnetic spring was studied using a ramping force test and electromagnetic simulation. A two-zone linear region, from 0° to 2° and 2° to 6.5°, was observed and explained through magnetic flux simulation to provide insight into the fundamentals of the electromagnetic spring. An unusual impedance response was also noted from this regional linearity, appeared on a step gain in Bode plot of end-point impedance in a dynamic test.**

I. Introduction

The concept of a variable stiffness actuator (VSA) has attracted considerable attention for over two decades, particularly in robotics and automation fields [1]. Owing to its adjustable stiff feature, a VSA can balance safety and performance in several scenarios; for example, mitigating the impact from kicking or hammering [2], adjusting for periodic variances in walking trajectories [3], and facilitating safe training during neuro-rehabilitation [4]–[5]. These scenarios will soon be commonplace as robot technology develops. VSAs represent a potential method of satisfying two opposite conditions—namely, low stiffness but high fidelity and high stiffness but low force fidelity [6]—in a wide range of applications. Stiffness response is a key aspect of performance when the condition rapidly changes; for instance, altering assistive forces according to the needs of patients undertaking elbow training [7].

In general, VSAs can be classified into three major mechanisms in accordance with which components and properties are manipulated: (1) the mechanical preload on the springs, (2) the force ratio in transmission, and (3) the physical properties of the springs, for which detailed descriptions may be found in a review paper [8–9]. Stiffness changes associated with movement or deformation of components have been widely used in most VSA designs, such as spring deflecting, lever pivoting, and roller shifting. The response of related motions affects stiffness bandwidth. In contrast to kinetic approaches, use of changing magnetic fields can potentially enhance responses without concern for motion dynamics. An electromagnetic (EM) spring was first introduced in a VSA design [10]. In [10], various torque responses could be realized by varying the current applied to EM coils; however, the slope of the response curve suddenly declined at a rotation angle of approximately 2°. Two linear regions within 6.5° were observed and regarded as a challenge in controlling the actuator. This phenomenon, based on magnetic flux, differs from the fundamental principle of spring deflection; however, investigation in two-zone linear regions has not yet been conducted.

In this study, a basic idea and design of EM spring was illustrated. Ramping force and sweeping angle tests were performed to identify the static and dynamic characteristics, respectively, of the EM springs. The stiffness within two linear zones was investigated to characterize each EM spring at several currents. Finally, magnetic flux simulation results explained why the response curve's slope drops at a specific angle.

II. Principle and Concept

A. Using Magnetic Flux as a Spring

Magnets tend to produce magnetic fields, pulling in ferromagnetic materials such as iron and steel and attracting or repelling other magnets. This natural phenomenon provides a driving force; in fact, magnet springs with magnet–magnet combinations have been used as passive element—for example, in vehicle suspension [11] and vibration isolation [12]—and an electromechanical model has also been developed [13] for this design.

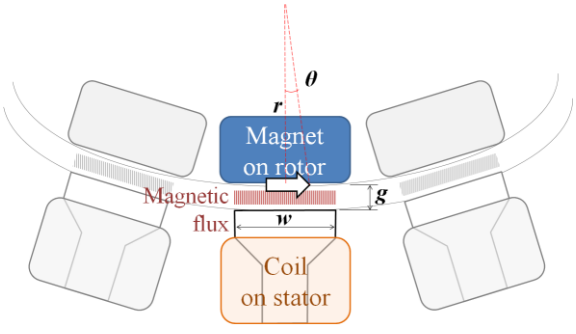

Fig. 1 EM spring concept

*Resrach supported by Ministry of Economic Affairs, R.O.C. (Taiwan)

H. -P. Yang is with the Mechanical and Mechatronics Systems Research Laboratories, Industrial Technology Research Institute, 31057 Hsinchu, Taiwan (corresponding author to provide phone: +886-3-5915922; fax: +886-3-5910324; e-mail: hanping_yang@itri.org.tw).

C. -S. Jang, is also with the Mechanical and Mechatronics Systems Research Laboratories, Industrial Technology Research Institute, 31057 Hsinchu, Taiwan (e-mail: CSJang@itri.org.tw).

H. van der Kooij is with Department of Biomechanical Engineering , Faculty of Engineering Technology, University of Twente, 7500 AE Enschede, The Netherlands, and with the Department of Biomechanical Engineering, Delft Technical University, 2600 AA Delft, The Netherlands (e-mail: h.vanderkooij@utwente.nl).

A basic set of an EM spring, composed of a magnet and a coil, is similar to a segment of an electric machine, as in Fig. 1. Magnetic flux flows from the magnet on the rotor to the coil with an iron core in the stator; it then backs through the adjacent EM spring couples. Its torque response can be treated as cogging torque T_{cog} in an electric machine and thus, for this rotational case involving a mutually coupled magnet and coil given by [14]

$$T_{cog} = -\frac{1}{2}\phi^2 \frac{dR}{d\theta} \tag{1}$$

where ϕ is magnet flux crossing the air gap, θ is angle of rotation, and R is total reluctance through the flux pathway. To consider the dimensions indicated in Fig. 1, total reluctance R can be rewritten as

$$R = \frac{g}{\mu_0 wL} \tag{2}$$

where g is the air gap between the rotor and the stator, μ_0 is the permeability of free space ($4\pi \times 10^{-7}$ H/m), w is the tooth width, r is the rotor radius, and L is the thickness of the rotor and stator. Applying (2) in (1), torque response T is given by

$$T = -\frac{1}{2}\phi^2 \frac{gr}{\mu_0 L} \frac{1}{(w - r\theta)^2} \tag{3}$$

This equation illustrates that the torque is affected by the magnet flux and angle of rotation. When the magnet flux is constant, torque response is approximately linear for small rotation angles. However, torque response can be dramatically influenced by magnet flux; thus, torque response or EM spring stiffness can be regulated by the applied current.

B. EM Spring Module

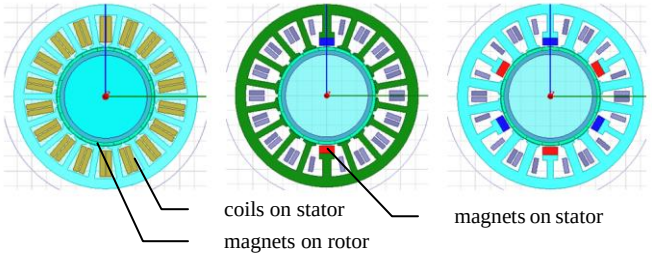

Type 0	Type 1	Type 3
Rotor: 18 magnets Stator: 18 coils	Rotor: 18 magnets Stator: 2 magnets 16 coils	Rotor: 18 magnets Stator: 6 magnets 12 coils

Fig. 2 Three EM spring module arrangements.

To investigate characteristics in the module level, three types of EM spring were prepared, as in Fig. 2. Type 0 was designed as a pure EM module, meaning that no magnet was placed on the stator. In total, 18 magnets and coils were placed evenly on the rotor and stator, respectively. Type 1 and 3 replaced two and six coils on the stator with magnets; consequently, they achieved higher stiffness than Type 0 and maintained their stiffness without any current. Their overall dimensions were the same and they could be easily interchanged. For the winding, coils were serially connected, and winding direction was alternated with adjacent coils to be individually aligned with the rotor magnets.

C. EM Spring VSA Design

In response to high demand for lightweight and small pieces of robotic equipment, a compact EM spring VSA was originally developed for a rehabilitation exoskeleton robot [10]. Fig. 3(a) depicts the concept of actuator architecture where the position motor and EM spring are individually coupled to differential gear to create a physical series connection. Fig. 3(b) depicts the corresponding structural arrangement. As illustrated, the differential gear was located in the center of the EM spring and position motor to create an extremely compact module with dimensions within 124 mm for the diameter and 55 mm for the thickness.

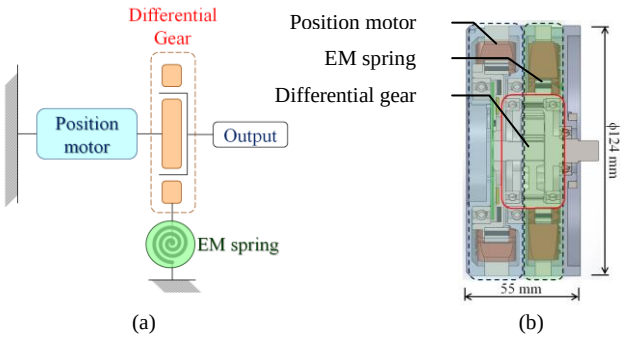

Fig. 3 EM spring VSA design. (a) Connection between components. (b) Component arrangement and structure design.

I. Prototypes and Experiment Setup

Two experiments, one for ramping force and the other a sweeping angle test, were assigned to identify the EM spring characteristics. In the ramping test, the position of position motor in the VSA prototypes was fixed by either applying a servo position command or jamming a brake on the rotor to eliminate force coupling. An external ramping force was applied on the output shaft until the EM spring rotor jumped away from original position, whereupon torque response and rotation angle were recorded simultaneously by an external torque and position sensor. In the same manner, the sweeping angle test also required the position motor to be in a fixed position; a reciprocating angle was then applied to the EM spring instead of a ramping force.

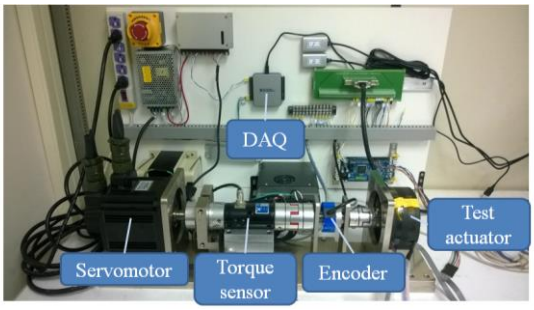

Fig. 4 Experimental setup

The experimental setup was established for the aforementioned tests is seen in Fig. 4. A commercial servo motor (Delta ECMA-G21309) was used as an external load to

generate a ramping force and sweeping angle. Torque sensor (Esense RT-10) was located at the output shaft of this servomotor along with an encoder (Tamagawa OIH60-8192P). The VSA was connected to the encoder. All the control procedure and signal processing were handled by a DAQ (NI USB-6003) and the LabVIEW software.

II. Test and Simulation Results

Type 1 EM spring had a unique role among these three types because of one-magnet-pair arrangement which meant that both the characteristics of the magnet and pure EM could be observed in the test results. The findings therefore focus on these results.

A. *Static Stiffness Test by Ramping Force*

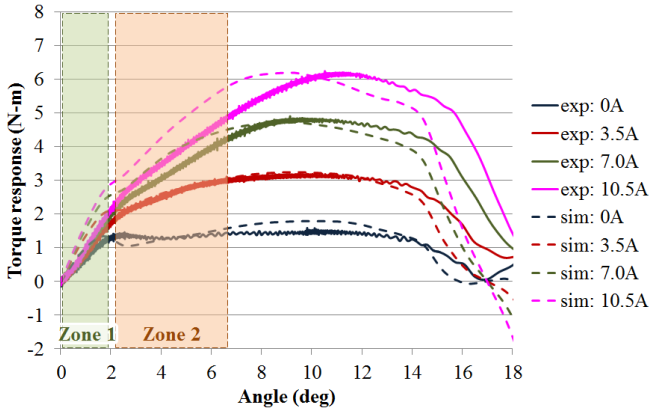

Fig. 5 Experiment (solid lines) and simulation results (dotted lines) of the ramping force test at different currents (Type 1 EM spring). The green shaded region, zone 1 covers the first linear section of the torque response; the brown region, zone 2, covers the second linear region of the response curve.

In this test, the external load was slowly raised at 0.15 N-m/s. Four currents from 0 to 10.5 A were applied to the EM spring, and corresponding finite element simulation was conducted using ANSYS Maxwell; the comparison can be seen in Fig. 5. As shown, all of the torque response curves have similar patterns and vary by applied current; the stiffness can be derived from the slope of the response curve. Two linear zones, from 0°–2° (zone 1) and 2°–6.5° (zone 2), are highlighted in the green and brown shaded regions of Fig. 5; that is, the EM spring maintains constant stiffness within these two regions. The maximum torque, the so-called holding torque, appeared at approximately 10° and could achieve up to 6 N-m at 10.5 A. At greater torques, the rotor of the EM spring jumped away from the originally aligned tooth in the test. For the simulation results (dotted lines), a similar trend emerged as for the experiment results at all currents. The maximum torques were close to the test results. This finding revealed high accuracy for the simulation and inspired us to explore the behaviors of EM spring by means of simulation.

To understand the behavior of the magnetic field in the EM spring at different angle, the magnetic flux flow charts were inspected. As indicated in the red circles in Fig. 6, a local flux loop was initiated at the edge of the tooth from 2° and kept increasing from 3° to 5°. This local flux loop gradually interfered with the magnetic flux crossing the air gap; consequently, the torque response slope started to decline.

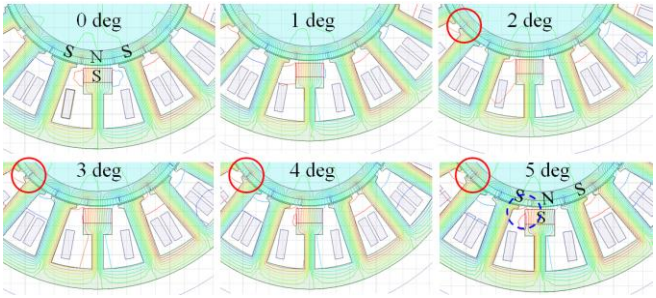

Fig. 6 Simulation results of magnetic flux flow at different angle (Type 1 EM spring at a current of 10.5A). The red circle indicates that a local flux loop occurred at the edge of the tooth. The blue dotted circle indicates the flux distortion around the edge of the magnet.

In contrast to the local flux loop occurring at the edge of the tooth, the magnet on top of the tooth produced an opposing flux manner on the stator. At 0° in Fig. 6, the magnets on rotor and stator were well aligned, with most of the flux flowing from the N to S pole through the air gap; however, at 5° the rotor magnet (S pole) rotated to face the magnet (S pole) on the stator. The flux line distorted at the edges, as indicated in the blue dotted circle in Fig. 6; therefore, the attractive force between the N–S pole pair decreased, and repelling force (S–S pole) increased. The growth and decline between these two forces caused the torque response to fluctuate within a certain level, denoted by the 0 A curve in Fig. 5.

The slope for torque response (i.e. stiffness) within the two linear zones in Fig. 5 is given in detail in Table. I.

TABLE I. Stiffness within the Two Linear Zones (Type 1)

	ZONE 1: 0 - 1 deg		ZONE 2: 3 - 6 deg	
	(N-m/deg)	(db)	(N-m/deg)	(db)
0 A	0.859	-1.32014	0.0612	-24.265
3.5 A	1.1547	1.249383	0.2136	-13.408
7 A	1.4129	3.002229	0.4639	-6.67151
10.5 A	1.5045	3.547844	0.5587	-5.05643

B. *Dynamic Stiffness Test by Sweeping Angle*

In this test, a back-and-forth motion command with a sine sweep trajectory from 1 to 100 Hz with two amplitudes of 2° and 8° was set as the target position for the servo motor. Both the time and frequency domain results are shown in Fig. 7. In the chart for 2° amplitude, the end-point impedance approximately 3.5 db and bandwidth at approximately 50 Hz were obtained using a Bode plot. The value matched with the static stiffness at 10.5 A in Table. I. However, the trend in frequency response for the 8° amplitude was slightly different than for the 2°. The gain oscillated around 0 db from 1 to 5 Hz and then rose to 3.5 db. To compare this with time domain response, the angle entered zone 2 before 0.5 s, which was approximately 5 Hz in the Bode plot; thus, the gain was between 3.5 and −5 db. When the angle stayed in zone 1, the gain instantly returned to 3.5 db.

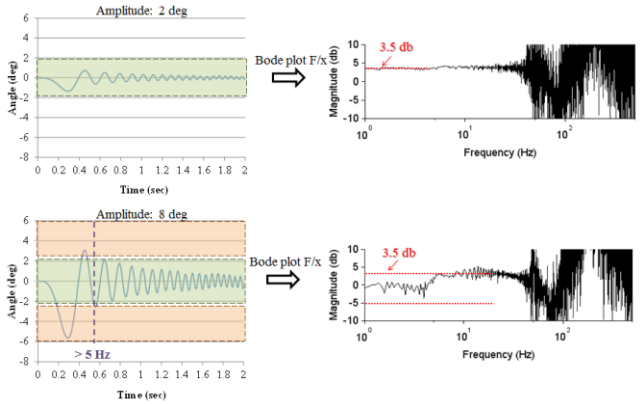

Fig. 7 Experimental results and Bode plot of the sweeping angle tests (Type 1 EM spring for a current of 10.5A).

III. Discussion and Conclusion

This paper outlined the concept of an EM spring, and three types of EM springs were briefly described to provide a preliminary impression of this new VSA design. In the study, the characteristic two-zone linear region of torque response to rotations was examined using experiments and simulation with a ramping force and a sweeping angle test. Previously, the static stiffness of an EM spring at different currents has been obtained. Simulation results reveals that a local flux loop was initiated at the tooth edge from 2°, resulting in observed stiffness decline at approximately 2°. A flux distortion at the magnet edge could also be seen in the simulation results. These results suggested that local flux change from geometric rotation caused the two-zone linear phenomenon. Therefore, the design key points would be (1) shaping the teeth and magnets to manipulate the local flux, and (2) tuning rotor magnet spacing and width ratio between the magnets and teeth to expand the first linear zone. However, the rotation angle in dynamic tests must be controlled to avoid complex results associated with zone 1 and zone 2. In force-sensitive applications, namely rehabilitation, the rotation angle should be limited within zone 1 to conduct linear torque response.

In summary, EM springs have unique features and capabilities, namely rapidly modulation of stiffness, compact size, lack of requirement for mechanical motions, and potential to fulfill emerging needs for faster, smaller VSAs. In the future, the analytical model for the geometry of EM springs' magnets and teeth will be studied to provide a design reference. The related dimensions for the magnet and the tooth can be obtained according to design requirement, and the linear regions can be estimated in the design phase. The aim is to achieve higher stiffness response with the proposed EM spring–based VSA.

Appendix

Three VSA prototypes with Type 0, 1, and 3 EM springs were constructed for the characterized experiment, as seen in Fig. A1. All EM spring types could be interchanged with each other in the actuator module because the dimensions were equal and the mechanical interface shared the same design.

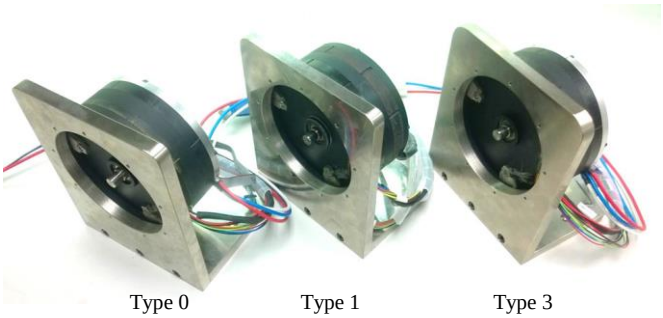

Fig. A1 Three EM spring VSA prototypes.

Acknowledgment

This research work was supported by the Ministry of Economic Affairs, R.O.C. (Taiwan) as a part of the research program for Interactive Rehabilitation Technology of Exoskeleton Robot from 2013 to 2016. Authors would like to express our appreciation to motor team in ITRI for prototype preparation and experiment setup, including Jih-Yang Chang, Hsin-Tien Yeh and Tsu-Min Liu. This work also gets help from Dr. Shang-Hsun Mao (Taiwan ANSYS Tech. Co.) for simulation consulting, and Jessica Norris and Edward Moon (Wallace Academic Editing) for English style review. The authors gratefully acknowledge all their assistance and contribution to this paper.

References

[1] G. Grioli, *et al*. "Variable Stiffness Actuators: The User's Point of View." *The International Journal of Robotics Research*, vol. 34, no. 6, May 2015, pp. 727–743, doi:10.1177/0278364914566515.

[2] M. Garabini, A. Passaglia, F. Belo, P. Salaris and A. Bicchi, "Optimality principles in variable stiffness control: The VSA hammer," *2011 IEEE/RSJ International Conference on Intelligent Robots and Systems*, San Francisco, CA, 2011, pp. 3770-3775, doi: 10.1109/IROS.2011.6094870.

[3] L. C. Visser, R. Carloni and S. Stramigioli, "Energy Efficient Control of Robots with Variable Stiffness Actuators," *IFAC Proceedings Volumes*, vol. 43, I. 14, 2010, pp. 1199-1204, doi: 10.3182/20100901-3-IT-2016.00241.

[4] J. F. Veneman, R. Kruidhof, E. E. G. Hekman, R. Ekkelenkamp, E. H. F. Van Asseldonk and H. van der Kooij, "Design and Evaluation of the LOPES Exoskeleton Robot for Interactive Gait Rehabilitation," *IEEE Transactions on Neural Systems and Rehabilitation Engineering*, vol. 15, no. 3, Sept. 2007, pp. 379-386, doi:10.1109/TNSRE.2007.903919.

[5] S. Zhang, S. Guo, M. Pang, B. Gao and P. Guo, "Mechanical Design and Control Method for SEA and VSA-based Exoskeleton Devices for Elbow Joint Rehabilitation," *Neuroscience and Biomedical Engineering*, vol. 2, I. 3, 2014, pp. 142-147, doi: 10.2174/2213385203666150514235041.

[6] H. Yu, S. Huang, G. Chen and N. Thakor, "Control design of a novel compliant actuator for rehabilitation robots," *Mechatronics*, vol. 23, I. 8, 2013, pp.1072-1083, doi: 10.1016/j.mechatronics.2013.08.004.

[7] J. Choi, C. Son, S. Park, E. Jung and D. Yu, "Elbow training device using the Mechanically Adjustable Stiffness Actuator(MASA)," *2018 40th Annual International Conference of the IEEE Engineering in Medicine and Biology Society (EMBC)*, Honolulu, HI, 2018, pp. 3614-3617, doi: 10.1109/EMBC.2018.8512984.

[8] S. Wolf, *et al.*, "Variable Stiffness Actuators: Review on Design and Components," *IEEE/ASME Transactions on Mechatronics*, vol. 21, no. 5, Oct. 2016, pp. 2418-2430, doi: 10.1109/TMECH.2015. 2501019.

[9] B. Vanderborght, *et al.*, "Variable impedance actuators: A review," *Robotics and Autonomous Systems*, vol. 61, I. 12, 2013, pp 1601-1614, doi: 10.1016/j.robot.2013.06.009.

[10] J. Chang, H. Yang, C. Jang, H. Yeh and T. Liu, "A new compliant actuation: Electromagnetic spring uses in parallel elastic actuator," *2016 16th International Conference on Control, Automation and Systems (ICCAS)*, Gyeongju, 2016, pp. 1549-1552, doi: 10.1109/ICCAS.2016.7832509.

[11] Y. Jia, S. Li and Y. Shi, "An Analytical and Numerical Study of Magnetic Spring Suspension with Energy Recovery Capabilities," *Energies*, vol. 11, I. 11, 2018, pp. 3126, doi: 10.3390/en11113126.

[12] J. Snamina and P. Habel, "Magnetic Spring as The Element of Vibration Reduction System," *Mechanics and Control*, vol. 29, no.1, 2010, pp. 40-44.

[13] M. Novak, J. Cernohorsky and M. Kosek, "Simple Electro-Mechanical Model of Magnetic Spring Realized from FeNdB Permanent Magnets," *Procedia Engineering*, vol. 48, 2012, pp. 469-478, doi:10.1016/j.proeng.2012.09.541.

[14] D. C. Hanselman, *Brushless Permanent Magnet Motor Design*, 2nd ed., McGraw-Hill, Inc., 2003.